NASA Technical Memorandum 104411
AIAA-90-2460

A CFD Study of Jet Mixing in Reduced Flow Areas for Lower Combustor Emissions

C.E. Smith and M.V. Talpallikar
CFD Research Corporation
Huntsville, Alabama

and

J.D. Holdeman
Lewis Research Center
Cleveland, Ohio

Prepared for the
27th Joint Propulsion Conference
cosponsored by the AIAA, SAE, ASME, and ASEE
Sacramento, California, June 24-27, 1991

A CFD STUDY OF JET MIXING IN REDUCED FLOW AREAS FOR LOWER COMBUSTOR EMISSIONS

C. E. Smith*
M. V. Talpallikar**
CFD Research Corporation
Huntsville, AL 35805

J. D. Holdeman***
NASA Lewis Research Center
Cleveland, OH 44135

Abstract

The Rich-burn/Quick-mix/Lean-burn (RQL) combustor has the potential of significantly reducing NO_x emissions in combustion chambers of High Speed Civil Transport (HSCT) aircraft. Previous work on RQL combustors for industrial applications suggested the benefit of "necking down" the mixing section. In this study, a 3D numerical investigation was performed to study the effects of neckdown on NO_x emissions and to develop a correlation for optimum mixing designs in terms of neckdown area ratio. The results of the study showed that jet mixing in reduced flow areas does not enhance mixing, but does decrease residence time at high flame temperatures, thus reducing NO_x formation. By necking down the mixing flow area by four, a potential NO_x reduction of sixteen-to-one is possible for annular combustors. However, there is a penalty that accompanies the mixing neckdown: reduced pressure drop across the combustor swirler. At conventional combustor loading parameters, the pressure drop penalty does not appear to be excessive.

1. Introduction

The design of low NO_x combustors is a subject of ongoing research at NASA Lewis Research Center as applied to High Speed Civil Transport (HSCT) aircraft. One combustor design presently under study is the Rich-burn/Quick-mix/Lean-burn (RQL) combustor. Originally conceived and developed for industrial combustors[1-2], the RQL concept utilizes staged burning, as shown in Figure 1. Combustion is initiated in a fuel rich zone at equivalence ratios between 1.2 and 1.8, thereby reducing NO_x formation by depleting the available oxygen. Bypass air is introduced in a quick-mix section and lean combustion occurs downstream at equivalence ratios between 0.5 and 0.7. A key design technology required for the RQL combustor is a method of rapidly mixing bypass air with rich-burn gases. Rapid and uniform mixing is required for producing low amounts of NO_x while oxidizing CO produced in the rich-burn section.

Generic research on dilution jet mixing in gas turbine combustors has been performed in the past[3], and is applicable to RQL combustors. Good

* Manager, Application Projects
Member AIAA
** Project Engineer
Member AIAA
*** Senior Research Engineer
Member AIAA

engineering correlations were developed for optimum mixing of dilution jets in can, rectangular and annular geometries[4]. In search of improved mixing schemes, recent work has been performed on staggered dilution jets in rectangular geometries[5], asymmetric jets in can geometries[6], and slots in can geometries[7].

An important aspect of jet mixing that warranted further investigation was the effect of "necking down" the mixing flow area. The mixing section has been typically necked down in RQL combustors to promote better mixing and prevent backflow[8-11]. In Reference 2 it was experimentally shown that neckdown of the mixing section produced lower NO_x emissions. The experiments did not provide the data base to identify why neckdown produced lower NO_x emissions or how to optimize NO_x reduction. Hence, this study was undertaken to investigate the effects of area reduction on NO_x formation in the mixing section, and to develop design correlations to optimize mixing in reduced areas.

2. Approach

Parametric numerical calculations were performed to quantify potential improvement from neckdown and to understand the physical mechanisms causing low NO_x. Both 3-D CFD numerical analysis and 1-D analysis were employed. The 3-D numerical calculations were made using the CFD code named REFLEQS. REFLEQS has been developed to analyze turbulent reacting flows[12], and has undergone a considerable amount of systematic quantitative validation for both incompressible and compressible flows. Over 30 validation cases have been performed to date, and good to excellent agreement between data and predictions has been shown[13-14]. Further, it has been shown that REFLEQS is a viable tool in modelling complex geometries and intricate flow patterns involved in mixing concepts of low emission combustors[5-7].

The study was divided into four parts. First, a baseline mixing configuration was analyzed and assessed for grid independence. Second, the baseline configuration was optimized in terms of number of slots. Third, a parametric variation of the mixing diameter (from six inches down to four inches) was performed to understand the cause of NO_x reduction in reduced flow area. And finally, a 1-D computer code was used to calculate the overall pressure loss of a combustor and to assess the penalty of mixing in a neckdown section. Each part of the study will be discussed in the following sections.

3. Baseline Case

Geometry

A "no neckdown" case was selected as the baseline. The baseline configuration (see Figure 2) consisted of three components: inlet pipe, converging section, and mixing section. The inlet pipe was 6.0 inches (0.152 m) in diameter and 3.0 inches (0.0762 m) in length. The convergence section connected the inlet pipe to the mixing section and was 0.866 inches (0.022 m) in length. The mixing section had a diameter of six inches (*i.e.* no neckdown) and had twelve equally-spaced slots located on its perimeter. The slots' centerlines were located one mixing section diameter downstream of the exit plane of the converging section. The aspect ratio of each slot was 4-to-1, with the largest dimension of 1.31 inches (0.033 m) positioned in the direction of the mainstream. The mixing section extended two mixing section diameters downstream of the jet centerline.

Grid

The baseline grid had 20,160 cells (56×20×18 cells in x, r, θ directions). Figure 3 shows two views of the baseline grid. The grid distribution is non-uniform with greater grid density in the vicinity of the slot as well as the combustor wall. The domain in the θ-direction extends from the jet centerline to between the jets. Only a pie section with a central angle of 15° was analyzed to conserve grid points. The grid distribution in each direction is described below.

Axial Direction

$X_0 < x < X_1$	inlet pipe	4 cells	uniform
$X_1 < x < X_2$	converging section	2 cells	uniform

$X_2 < x < X_3$	pre-slot	10 cells	matched last cell to the 1st cell in the slot
$X_3 < x < X_4$	slot	8 cells	uniform
$X_4 < x < X_5$	post-slot to 1-D	22 cells	matched 1st cell to last cell in the slot
$X_5 < x < X_L$	1-D to exit	10 cells	matched 1st cell to last cell of previous domain

Radial Direction

$R_0 < r < R_L$	20 cells	grid refined at the combustor wall with algebraic packing factor of 1.4

Angular Direction

$\theta_0 < \theta < \theta_1$ slot	6 cells	uniform
$\theta_1 < \theta < \theta_L$	12 cells	matched 1st cell with last cell in the slot

The values of the grid variables in the different zones discussed above are given in Table 1.

Table 1. Grid Data

Dia	6"	5"	4"
X_0	-0.2506	-0.2252	-0.1998
X_1	-0.1744	-0.1490	-0.1236
X_2	-0.1524	-0.1270	-0.1016
X_3	-0.0167	-0.0139	-0.0111
X_4	0.0167	0.0139	0.0111
X_5	0.1524	0.1300	0.1016
X_L	0.3048	0.2540	0.2032
R_0	0.0000	0.0000	0.0000
R_L	0.0762	0.0762	0.0762
θ_0	0.0000	0.0000	0.0000
θ_1	3.1400	3.1400	3.1400
θ_L	15.0000	15.0000	15.0000

Units
x ~ m
R ~ m
θ ~ deg

Numerical Details

The numerical details of the baseline calculation (as well as all calculations in this paper) included:

1. Wholefield solution of u momentum, v momentum, w momentum, pressure correction, turbulent kinetic energy (k), turbulence dissipation (ε), total enthalpy, and mixture fraction.
2. Second order central differencing of convective and diffusive fluxes;
3. Variable fluid properties;
4. Adiabatic walls;
5. Standard k-ε model with wall functions;
6. Turbulent Prandtl number of 0.9;
7. Instantaneous heat-release model and one-step NO_x model (details of the reaction models are discussed in reference 7); and
8. Six chemical species.

Boundary Conditions

The baseline case had a jet-to-mainstream momentum flux ratio (J) of 36 and a jet-to-mainstream mass flow ratio of 1.94. Specific boundary conditions are stated below.

Mainstream Flow

Axial Velocity	=	35.4 m/s (116.2 ft/s)
Temperature	=	2221 °K (3538 °F)
Density	=	1.864 kg/m^3 (0.1163 lbm/ft^3)
Composition (mass fraction)	=	0.134 CO, 0.068 CO_2, 0.006 H_2, 0.096 H_2O, 0.696 N_2
Turbulent kinetic energy, k	=	300.0 m^2/s^2 (3.2x10^3 ft^2/s^2)
Dissipation of turbulent kinetic energy, ε	=	5.5x10^5 m^2/s^3 (5.92x10^6 ft^2/s^3)

The mass fractions of the species were equilibrium concentrations for propane and air at an equivalence ratio (ϕ) of 1.6. The turbulent kinetic energy corresponded to a high turbulence intensity (40%) typically encountered at the exit of combustor primary zones[15]. However, the solution has been shown to be relatively insensitive to inlet turbulent kinetic energy.

Jet Flow (Slot)

Radial Velocity	=	120.3 m/s (394.6 ft/s)
Temperature	=	811 °K (1000 °F)
Density	=	5.82 kg/m^3 (0.36 lbm/ft^3)
Composition (mass fraction)	=	0.232 O_2, 0.768 N_2
Turbulent kinetic energy, k	=	219.0 m^2/s^2 (2.3x10^3 ft^2/s^2)
Dissipation of turbulent kinetic energy, ε	=	1.2x10^5 m^2/s^3 (1.3x10^6 ft^2/s^3)

The radial velocity corresponded to a liner $\Delta p/p$ of 0.03. The assumed turbulent kinetic energy gave a turbulence intensity of 10%, typical of dilution jets[15].

Exit Boundary

The exit boundary condition was a fixed pressure boundary with pressure set at 200 psia (13.6x10^5 N/m^2). All other variables (velocity components, physical properties, turbulence variables, species concentrations, *etc.*) were zero gradient.

Transverse Boundaries

The transverse boundaries were assumed to be symmetry planes. As a check for potential asymmetric and/or periodic flow behavior, the transverse boundaries were moved between slots (doubling the computational grid) and periodicity was enforced. No discernible difference was observed between the two solutions. Hence, to conserve grid points, transverse boundaries were assumed to be symmetric, and positioned on the jet centerline and between jets.

Combustor Wall

The combustor wall was treated as a no-slip adiabatic wall (zero enthalpy gradient). Wall functions were used for the calculation of wall shear stress and near wall turbulent quantities (k and ε).

Centerline

The computational boundary at the centerline was assumed to be a symmetry plane.

Convergence

The summations of all error residuals were reduced five orders of magnitude, and continuity was conserved in each axial plane. Typically, convergence required approximately 300 iterations. Approximately 6 CPU hours were required on an Alliant FX/8 mini-supercomputer (configured one computational element per job). For comparison, the Alliant computer speeds are ~20 times slower than a Cray X-MP.

Results for Baseline Case

The calculated isotherm results are presented in Figure 4. Figure 4a shows isotherms in the x-r plane through the center of the slot (θ = 0). Although a 15° pie section was numerically analyzed, the results in Figure 4 are shown as a 30° pie section for ease of understanding. The cold jet has penetrated to about the center of the mixing section. Reaction is taking place at the interface of the two flowstreams as evidenced by isotherms near stoichiometric temperature. At x/D=0.15, Figure 4b shows kidney-shaped isotherms behind the jet. Figure 4c shows the velocity vectors at x/D=0.5. The velocity vectors show the vortex roll-up behind the jet which is a typical feature of a jet in crossflow.

In Figure 5, NO_x emissions are presented in terms of NO_x Emission Index (EI) as a function of axial distance. NO_x EI is derived from the sum of volume fractions of NO and NO_2, and expressed as equivalent grams of NO_2 per kilogram of fuel. The value of NO_x EI one diameter downstream of the jet centerline (x/D=1.0) is 8.14.

4. Grid Independence Study

Two sizes of grids were employed to check for grid independence. The baseline grid was 20,160 cells and the fine grid was 68,040 cells. The fine grid was obtained by increasing the grid density by 50% in each of the three directions and maintaining the same stretching factors.

Computational results for the two grids are presented in Figure 6. Quantitatively, they are nearly the same. However, the fine grid solution shows slightly greater jet penetration and less temperature dissipation.

To estimate numerical error caused by grid resolution, the Richardson extrapolation method was employed. The Richardson extrapolation method utilizes a Taylor series expansion on the baseline and fine grid solutions to obtain an approximate solution based on zero discretization error. The values of NO_x EI at x/D=1.0 are 8.14, 7.97, and 7.47 for the baseline grid, fine grid and zero error grid, respectively. Based on this finding, hundreds of thousands of grid cells would be required to obtain a grid independent solution. Such fine grids were not practical in this study. For a comparative study such as this, it was felt the baseline grid is sufficient in accuracy, and should give qualitative engineering answers.

5. Optimization on Number of Slots

It has been shown in the past[16-19] that temperature distributions are similar when J and orifice spacing are coupled. Since the number of orifices follows from orifice spacing, optimum mixing in a can occurs when the following expression is satisfied[4]:

$$n = \frac{\pi\sqrt{2J}}{C} \qquad (1)$$

where

n = optimum number of holes
C = experimentally derived constant ~ 2.5
J = jet-to-mainstream momentum flux ratio

Using equation 1, the optimum number of slots would be 10 or 11 depending on the roundoff. However, this correlation was developed for circular holed dilution jet mixing and jet-to-mainstream mass flow ratios (m_j/m_∞) of approximately 0.5. The accuracy of equation 1 for high aspect ratio slots (4-to-1) and high mass flow ratios (1.94) studied in this investigation is not certain.

Hence, as a preliminary step to studying flow area reduction on mixing, a parametric study was performed to determine the optimum number of slots for J=36. The number of slots was parametrically varied from 10 to 14 on the baseline geometry. As the number of slots was varied, the central angle of the pie section changed, but the jet-to-mainstream mass flow ratio (m_j/m_∞) was held constant by varying the slot open area. The slot aspect ratio was maintained at 4 for all cases.

The same number of grid cells was used in all cases, including the number of grid cells in the slot. However, since the slot width-to-transverse dimension varied in each case, cell density in the θ-direction varied between cases. This variation is thought to have minimal impact on the trends discussed below.

Figure 7 shows the predicted isotherms in the θ=0 plane for different numbers of slots. The jet penetration increased as an inverse function of the number of slots and led to backflow as the number of slots was reduced to 10. From previous experience in reference 6, jet backflow on the mixing section centerline leads to poor mixing and excessive NO_x formation in the combustor. So, further decrease in number of slots below 10 was not considered necessary for this analysis. As the number of jets was increased to 14, the individual jets did not penetrate to the mixing section centerline. Such underpenetration has been shown to be poor from a mixing viewpoint.

Table 2 shows NO_x and CO emissions at x/D of 1.0 as a function of number of slots. NO_x emissions decrease with the increase in the number of slots. Going by NO_x emissions alone, the 14 slot case would be judged to be the optimum mixing configuration. However, for the 13 and 14 slot cases, CO has gone unreacted on the centerline of the mixer due to underpenetration of the dilution jets. The 12 slot configuration has the lowest NO_x EI while exhibiting no CO at x/D=1.0.

Based on this analysis, the 12 slot configuration was selected as the optimum mixer for this geometry and these flow conditions.

Table 2. NO_x and CO Emissions at x/D = 1 for Variable Number of Slots

Slots	NO_x EI	CO EI
10	10.07	0.00
11	8.73	0.00
12	8.14	0.00
13	7.37	1.22
14	6.75	5.71

6. Parametric Study of Area Reduction

Using the optimized 12 slot geometry, three neckdown configurations were analyzed to assess the effect of flow area reduction on NO_x emissions. The three mixing section diameters were 6, 5, and 4 inches (0.1524, 0.127, and 0.0762 m). As the flow area was reduced, the velocity of the mainstream flow in the mixing section increased proportionately to the flow area reduction. The resulting reduction in mainstream static pressure in the mixing section increased the pressure drop across the slots, thus increasing the jet velocity. For incompressible flow, the increase in mainstream and jet velocities exactly counterbalanced, and the jet-to-mainstream momentum flux ratio (J) remained constant as the mixing flow area was reduced.

The slot size was adjusted according to the variation in diameter of the mixing section to ensure a constant mass flow ratio (m_j/m_∞). The turbulence parameters at the jet inlet had to be rescaled according to slot size and the jet velocity. The jet velocity and turbulence parameters at the jet inlet for each mixing diameter are given in Table 3. The rest of the boundary conditions were the same as the baseline case except the exit boundary condition.

Table 3. Jet Velocity and Turbulence Data

Diameter	6"	5"	4"
V_j (m/s)	120.3	173.2	270.6
K_j (m^2/s^2)	219.0	454.1	1098.0
ε_j (m^2/s^3)	1.2×10^5	4.3×10^5	2.0×10^6

The pressure at the exit plane for the 6 inch diameter case was set to be 200 psia (13.6×10^5 N/m^2). For the 5 inch and 4 inch neckdown diameters, the exit pressure was set at 198.8 psia (13.52×10^5 N/m^2) and 195.3 psia (13.28×10^5 N/m^2), respectively. The lower pressures were determined by assuming isentropic flow expansion from the five or four inch diameter mixer to a 6 inch diameter exit. This precluded the necessity of modeling a diffuser at the exit of the five or four inch mixer in the CFD calculations.

The grid distribution in the axial and the radial direction was identical except for the size of the slot. The grid distributions for the three configurations are given in Table 1.

Figure 8 shows the isotherms in the plane through the jet centerline (θ=0) for all three cases. Figure 9 shows isotherms at an r-θ plane one mixing section diameter downstream of the jet inlet (x/D=1.0). In this figure, a full 360° plane is displayed, although the computations were performed on a 15° pie section. The identical nature of the flow patterns shows that the mixing characteristics were identical for each case.

There was some concern that flow separation was not predicted at the inlet to the four-inch diameter mixing section. To investigate this concern, a number of cases were run with fine grid in the converging section and immediately downstream. Cases were run with and without dilution jets. Without dilution jets, flow separation was predicted for laminar flow, but not for turbulent flow (although a somewhat thick boundary layer

was calculated downstream of the contraction). However, with dilution jets, the mainstream flow "sensed" the jet blockage and started accelerating at the entrance of the mixing section. Hence, flow separation (and a thick boundary layer) was avoided in the neckdown mixing sections.

In Figure 10, NO_x EI is plotted as a function of axial location for the three different neckdown diameters. NO_x decreased as the mixing section diameter decreased. For all the cases, CO was completely depleted by x/D of 1.0. The NO_x EI for the six inch diameter mixing section was 8.14 at x/D of 1.0, while the NO_x EI for the four inch diameter mixing section was 2.43, a 3.35-to-1 reduction.

The formation of NO_x is controlled by local temperature, local oxygen concentration, and local residence time. Since mixing was identical for the three mixing diameters analyzed, the local temperatures and oxygen concentrations must be identical. This left residence time as the parameter causing reduced NO_x levels. Residence time is reduced in neckdown mixers in two ways: higher velocities and shorter mixing lengths.

An engineering correlation was developed to approximate NO_x emissions attainable by reduced flow areas. The correlation (based on residence time considerations) is expressed below:

$$\frac{NO_{x\ neckdown}}{NO_{x\ no\ neckdown}} = \frac{A_{neckdown}}{A_{no\ neckdown}} \cdot \frac{H_{neckdown}}{H_{no\ neckdown}} \qquad (2)$$

where

A = flow area

H = height (diameter in can, duct height in annulus)

A comparison of CFD results with equation 2 is shown in Table 4.

Table 4. Neckdown Effect on NO_x Emissions

NO_x neckdown / NO_x no neckdown		
Neckdown Diameter	3-D Calculations	Eq. 2
6"	1.0	1.0
5"	1.73	1.75
4"	3.35	3.38

A flow area reduction of 4.0 appears to be possible in conventional combustor designs (see next section for details), giving a potential NO_x reduction of 16-to-1 in an annular combustor (8-to-1 in a can combustor).

7. 1-D Pressure Loss Analysis

There is a penalty involved in reducing the flow area of the mixing section. By necking down the mixing section, a total pressure drop occurs across the mixer, backpressuring the combustor. The backpressure causes a reduced pressure drop across the combustor swirler. The reduced swirler air pressure drop results in lower atomizing velocities and worse atomization quality.

To investigate this backpressure effect, a 1-D flow model of a combustor was developed. This model was similar to the 1-D model discussed in reference 2 that showed good agreement with experimental pressure loss measurements. Figure 11 shows the basic elements of the model, consisting of 1) primary zone section, 2) converging section, 3) constant-area mixing section, and 4) diffuser. The primary zone was six inches in diameter, and the mixing section diameter was varied between six and three inches.

The hot mainstream gases in the primary zone section were isentropically accelerated into the mixing section. In the mixing section, the 1-D momentum equation was used to solve for static pressure at the exit of the mixing section. The jet velocity was assumed to enter radially, and complete (*i.e.* uniform) mixing and reaction was assumed. An iterative solution procedure was used, in which the inlet pressure of the hot gases was iterated until a combustor exit pressure of 200 psia was attained.

To better understand the relationship of combustor loading parameter on backpressure penalty, calculations were performed with two reference velocities: 50 and 100 f/s. The reference velocity is defined as

$$V_{rel} = \frac{\dot{m}}{\rho A} \qquad (3)$$

where

$\dot{m}$ = total combustor airflow
ρ = combustor inlet density
A = area of the inlet (6 in. diameter)

A combustor reference velocity of 50 f/s corresponds to conventional combustor design practice.

Figure 12 presents the predictions of swirler pressure drop versus mixing flow area. For demonstration purposes, a six percent $\Delta p/p$ was assumed across the swirler for no mixing neckdown. As the mixing flow area was reduced, the pressure drop across the swirler was reduced. For a combustor reference velocity of 50 f/s, a 4-to-1 flow area reduction produced a four percent $\Delta p/p$ across the swirler. Such a swirler pressure drop should be acceptable to combustor designers. However, for a combustor reference velocity of 100 f/s, it is evident that excessive backpressure would result, making the three-inch diameter mixing design impractical.

To get confidence in the 1-D model, results from the 3-D CFD calculations were compared with the 1-D predictions. Figure 13 shows the comparison and good agreement between 1-D and 3-D calculations.

8. Conclusions

The overall conclusions of this study are :

1. By reducing residence time at high flame temperatures, mixing in a "neckdown" mixing section significantly reduces NO_x formation. A design correlation was developed for NO_x reduction attainable by area reduction, as shown in equation 2.

   Area reduction of 4.0 appears to be possible in conventional combustor designs, giving a potential NO_x reduction of 16-to-1 in an annular combustor (8-to-1 in a can combustor).

2. The penalty for neckdown manifests itself in reduced pressure drop across the combustor swirler. This backpressure effect is caused by increased total pressure loss across the mixing section. Analysis showed the penalty for neckdown to be relatively minor for conventional combustor loading parameters.

9. Acknowledgements

The authors wish to thank NASA Lewis Research Center for funding this work under NASA Contract NAS3-25967. Our thanks also are extended to Ms. Kathy W. Rhoades for preparing this typescript.

10. References

1. Mosier, S.A., and Pierce, R.M., "Advanced Combustion Systems for Stationary Gas Turbine Engines," Vol. I, EPA Contract 68-02-2136, 1980.
2. Pierce, R.M., Smith, C.E., and Hinton, B.S., "Advanced Combustion Systems for Stationary Gas Turbine Engines," Vol. III, EPA Contract 68-02-2136, 1980.
3. Holdeman, J.D., "Summary of NASA-Supported Experiments and Modeling of the Mixing of Multiple Jets with a Confined Crossflow for Controlling Exit Temperature Profiles in Gas Turbine Combustors," AIAA Paper 91-2458, 1991.
4. Holdeman, J.D., Srinivasan, R., and White, C.D., " An Empirical Model of the Effects of Curvature and Convergence on Dilution Jet Mixing", AIAA Paper 88-3180 (NASA TM 100896), July 1988.
5. Smith, C.E., "Mixing Characteristics of Dilution Jets in Small Gas Turbine Combustors," AIAA-90-2728,1990.
6. Talpallikar, M.V., Smith, C.E., and Lai, M.-C., "Rapid Mix Concepts for Low Emission Combustors in Gas Turbine Engines," NASA CR-185292, 1990.
7. Talpallikar, M.V., Smith, C.E., Lai, M.-C., and Holdeman, J.D., "CFD Analysis of Jet Mixing in Low NO_x Flametube Combustors," *36th* ASME International Gas Turbine and Aeroengine Conference, 1991.
8. Russell, P.L., *et al.*, "Evaluation of Concepts for Controlling Exhaust Emissions from Minimally Processed Petroleum and Synthetic Fuels," ASME Paper 81-GT-157, 1981.

9. Rosfjord, T.J., "Evaluation of Synthetic-Fuel-Character Effects on Rich-Lean Stationary-Gas-Turbine Combustion Systems, Vol. 1: Subscale Test Program," EPRI-AP-2822-Vol-1, 1981.
10. Novick, A.S., and Troth, D.L., "Low NO_x Heavy Fuel Combustor Concept," NASA CR-165367, 1981.
11. Lew, H.G., Carl, D.R., Vermes, G., DeZubay, E.A., "Low NO_x Heavy Fuel Combustor Concept Program, Phase 1: Combustion Technology Generation," NASA CR-165482, 1981.
12. Przekwas, A.J., Habchi, S.D., Yang, H.Q., Avva, R.K., Talpallikar, M.V., and Krishnan, A., "REFLEQS-3D: A Computer Program for Turbulent Flows With and Without Chemical Reaction, Volume 1: User's Manual," CFD Research Corp., Huntsville, AL, CFDRC Report GR-89-4, 1990.
13. Smith, C.E., Ratcliff, M.L., Przekwas, A.J., Habchi, S.D., and Singhal, A.K., "Modeling of Turbulent Combustion in Liquid Rocket Engine Components," NASA Contract NAS8-37619, 1988.
14. Smith, C.E., Ratcliff, M.L., Przekwas, A.J., and Habchi, S.D., "Validation of an Advanced Turbulent Combustion Code: REFLEQS," *7th* ASME CFD Workshop, NASA MSFC, 1989.
15. Smith, C.E., Graves, C.B., Johnson, B.V., and Roback, R., "Advanced Fuel Injector Characterization," Phase I Design Report, Navy Contract N00140-83-8899, 1986.
16. Holdeman, J.D., Srinivasan, R., and Berenfeld, A., "Experiments in Dilution Jet Mixing," *AIAA Journal*, vol. 22, No. 10, Oct. 1984, pp. 1436-1443.
17. Holdeman, J.D., and Srinivasan, R., Modeling Dilution Jet Flowfields, *J. Propulsion and Power*, Vol. 2, No. 1, Jan-Feb 1986, pp 4-10.
18. Holdeman, J.D., Srinivasan, R., Coleman, E.B., Meyers, G.D., and White, C.D., "Effects of Multiple Rows and Non-Circular Orifices on Dilution Jet Mixing," *J. of Propulsion and Power*, Vol. 3, No. 3, May-Jun 1987, pp. 219-226.
19. Holdeman, J.D., Srinivasan, R., Reynolds, R., and White, C.D., "Studies of the Effects of Curvature on Dilution Jet Mixing", *J.of Propulsion and Power*, vol. 7 No. 2, Mar-Apr 1991.

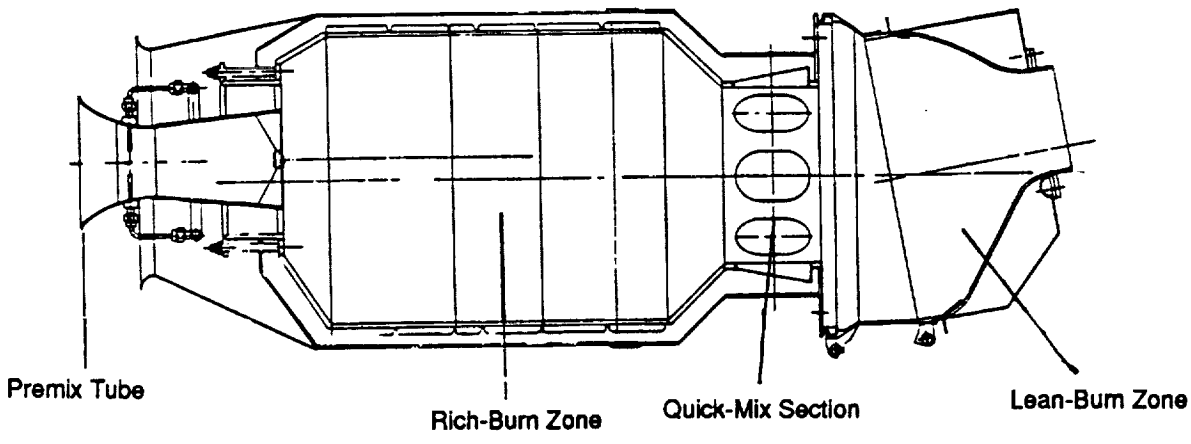

Figure 1. Industrial Rich/burn/Quick-mix/Lean-burn (RQL) combustor[2].

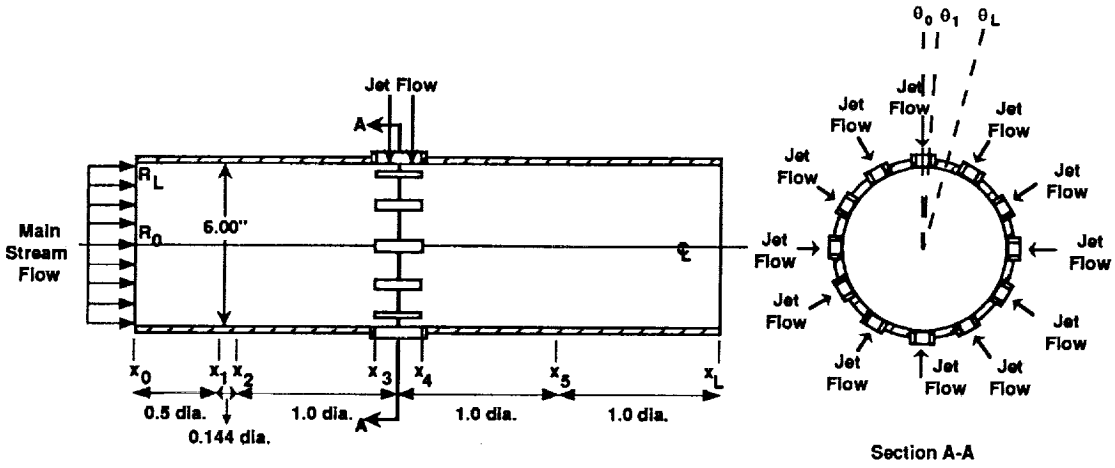

Figure 2. Schematic of baseline geometry.

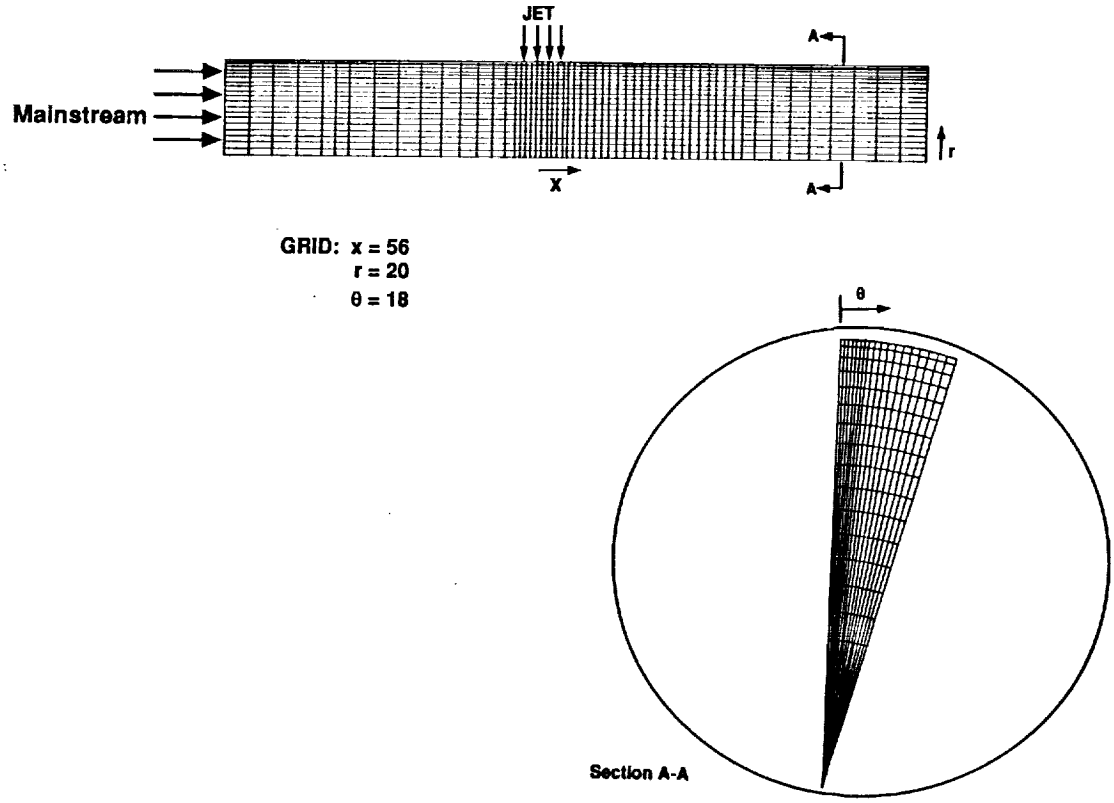

Figure 3. Numerical grid for baseline configuration.

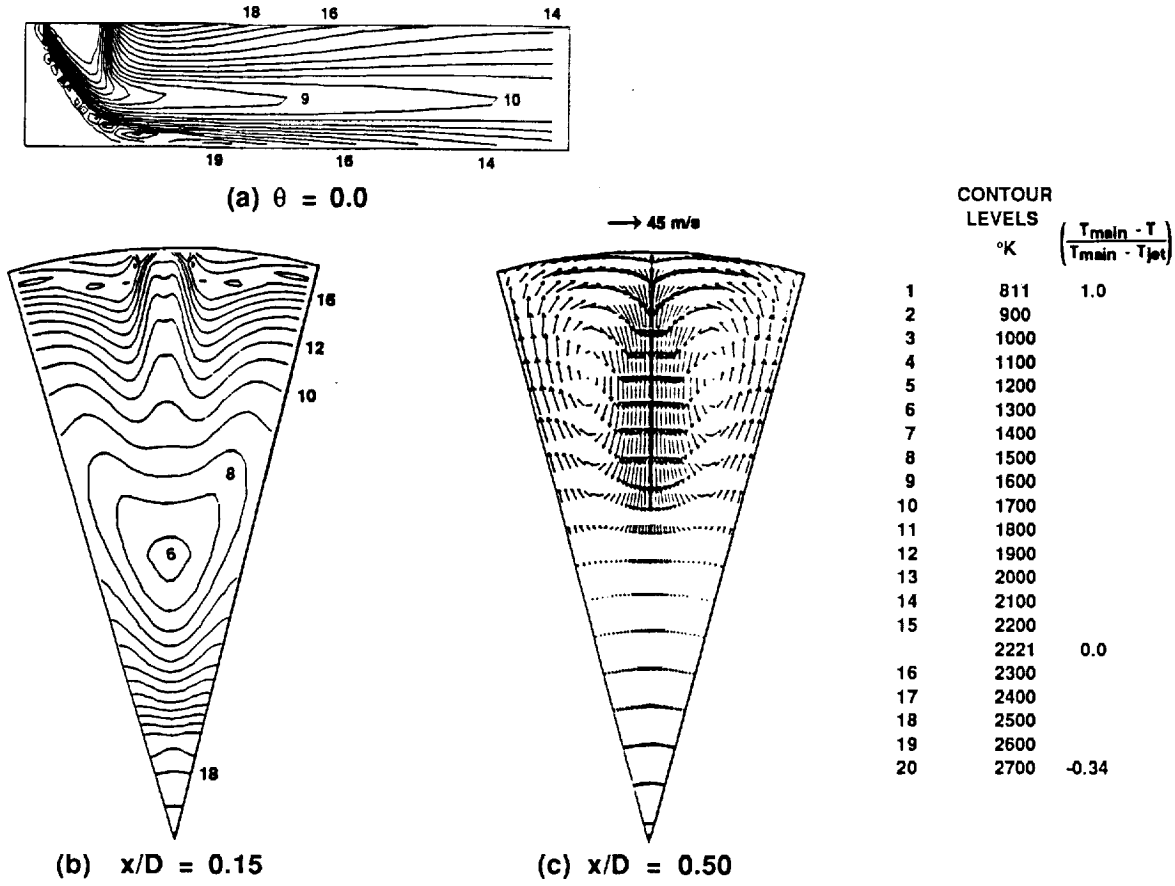

Figure 4. Computational results for baseline configuration.

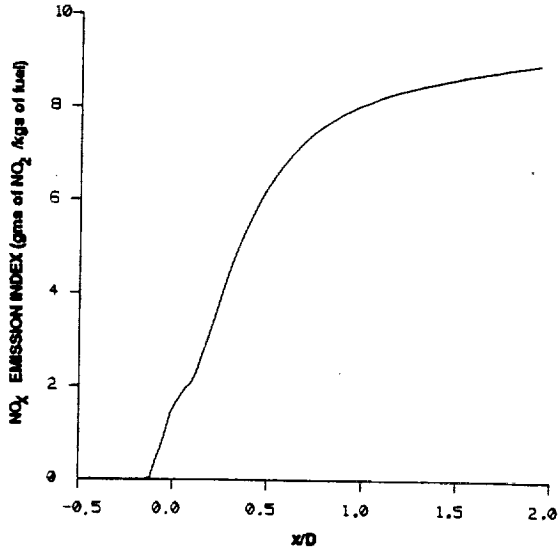

Figure 5. NO_x emission index for baseline configuration.

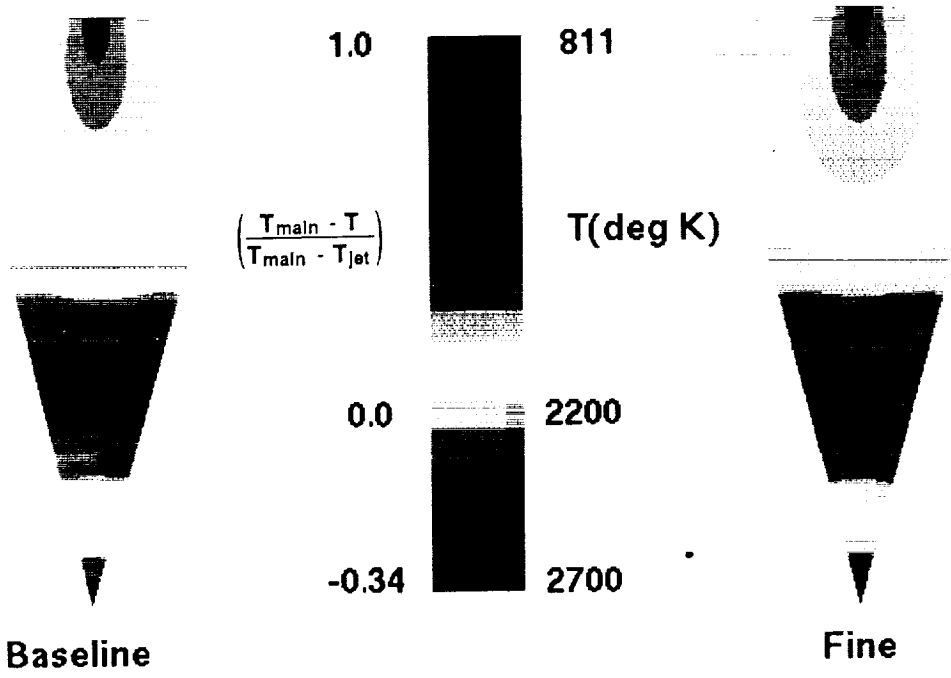

Figure 6. Isotherms predicted for baseline and fine grids: x/D=1.0.

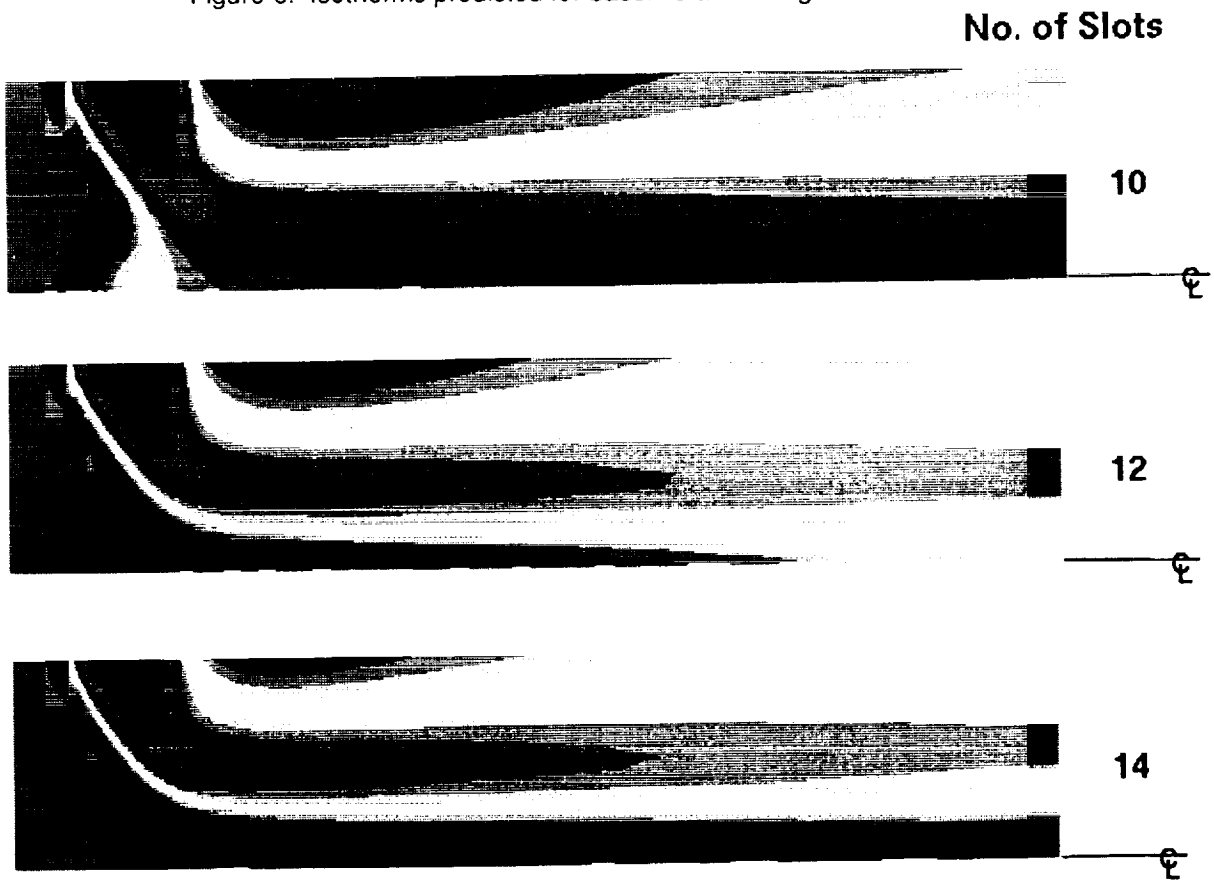

Figure 7. Predicted isothermal maps (θ=0) for J=36; variation in number of slots.
Temperature scale same as shown in Figure 8.

ORIGINAL PAGE
COLOR PHOTOGRAPH

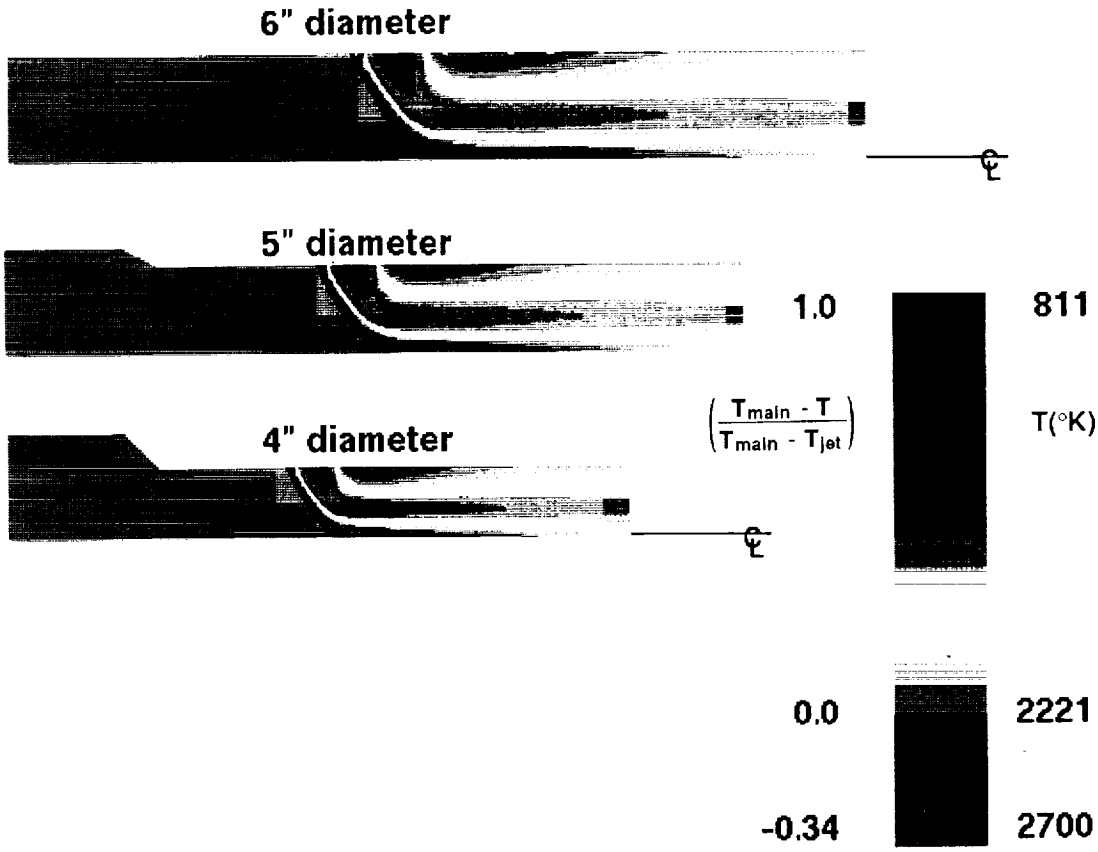

Figure 8. Predicted isothermal maps (θ=0) for J = 36; variation in mixing diameter.

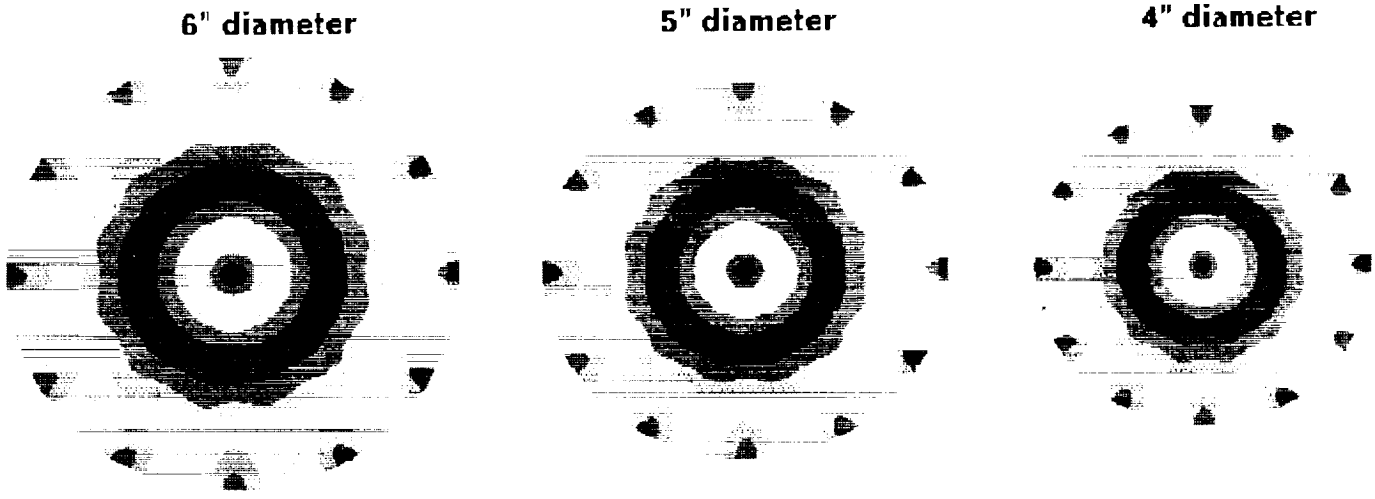

Figure 9. Predicted isothermal maps (x/D=1.0) for J=36; variation in mixing diameter.

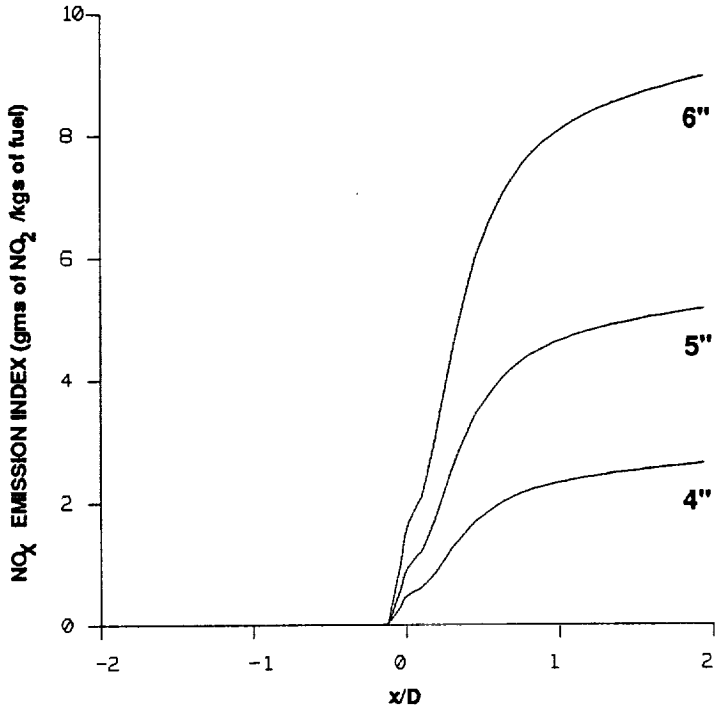

Figure 10. NO_x emission index for mixing diameters of 6", 5", and 4".

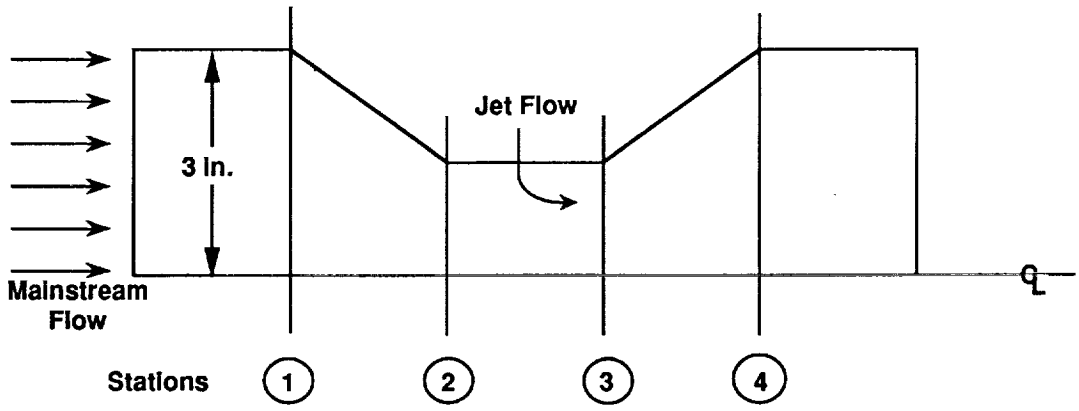

Figure 11. Schematic showing stations of 1-D pressure loss code.

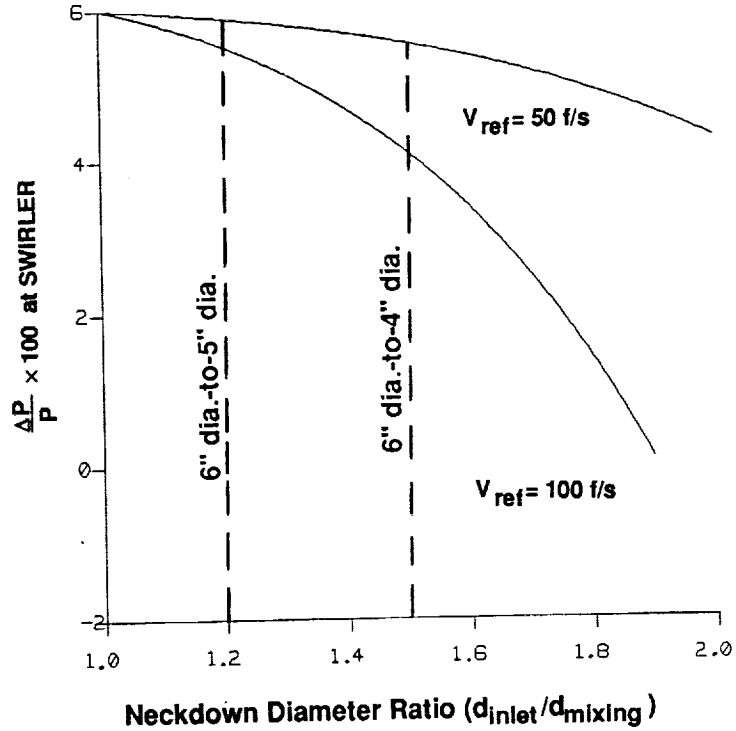

Figure 12. Percentage pressure drop available across the swirler as predicted by 1-D pressure loss code.

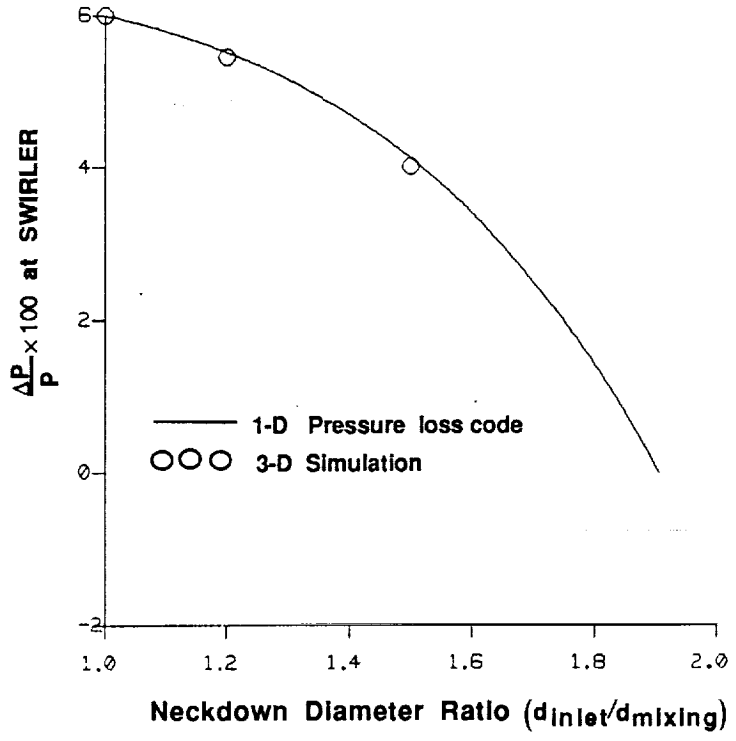

Figure 13. Pressure drop predicted by 1-D pressure loss code compared to 3-D calculations.

NASA
National Aeronautics and Space Administration

Report Documentation Page

1. Report No.	2. Government Accession No.	3. Recipient's Catalog No.
NASA TM-104411 AIAA-91-2460		

4. Title and Subtitle
A CFD Study of Jet Mixing in Reduced Flow Areas for Lower Combustor Emissions

5. Report Date

6. Performing Organization Code

7. Author(s)
C.E. Smith, M.V. Talpallikar, and J.D. Holdeman

8. Performing Organization Report No.
E -6238

10. Work Unit No.
537-02-21

9. Performing Organization Name and Address
National Aeronautics and Space Administration
Lewis Research Center
Cleveland, Ohio 44135-3191

11. Contract or Grant No.

13. Type of Report and Period Covered
Technical Memorandum

12. Sponsoring Agency Name and Address
National Aeronautics and Space Administration
Washington, D.C. 20546-0001

14. Sponsoring Agency Code

15. Supplementary Notes
Prepared for the 27th Joint Propulsion Conference cosponsored by the AIAA, SAE, ASME, and ASEE, Sacramento, California, June 24-27, 1991. C.E. Smith and M.V. Talpallikar, CFD Research Corporation, Huntsville, Alabama 35805 (work funded by NASA Contract NAS3-25967). J.D. Holdeman, NASA Lewis Research Center. Responsible person, J.D. Holdeman, (216) 433-5846.

16. Abstract
The Rich-burn/Quick-mix/Lean-burn (RQL) combustor has the potential of significantly reducing NO_x emissions in combustion chambers of High Speed Civil Transport (HSCT) aircraft. Previous work on RQL combustors for industrial applications suggested the benefit of "necking down" the mixing section. In this study, a 3D numerical investigation was performed to study the effects of neckdown on NO_x emissions and to develop a correlation for optimum mixing designs in terms of neckdown area ratio. The results of the study showed that jet mixing in reduced flow areas does not enhance mixing, but does decrease residence time at high flame temperatures, thus reducing NO_x formation. By necking down the mixing flow area by four, a potential NO_x reduction of sixteen-to-one is possible for annular combustors. However, there is a penalty that accompanies the mixing neckdown: reduced pressure drop across the combustor swirler. At conventional combustor loading parameters, the pressure drop penalty does not appear to be excessive.

17. Key Words (Suggested by Author(s))	18. Distribution Statement
Dilution; Can; Emissions; Jet mixing flow; Gas turbines; Combustion chamber	Unclassified - Unlimited Subject Category 07

19. Security Classif. (of the report)	20. Security Classif. (of this page)	21. No. of pages	22. Price*
Unclassified	Unclassified	22	A03

*For sale by the National Technical Information Service, Springfield, Virginia 22161